

THERMAL ANALYSES OF THE INTERNATIONAL
ULTRAVIOLET EXPLORER (IUE) SCIENTIFIC
INSTRUMENT USING THE NASTRAN
THERMAL ANALYZER (\bar{N} TA) - A GENERAL PURPOSE SUMMARY

Clifton E. Jackson, Jr.
Goddard Space Flight Center

SUMMARY

The \bar{N} TA (reference 1) Level 15.5.2/3, was used to provide non-linear steady-state (NLSS) and non-linear transient (NLTR) thermal predictions for the International Ultraviolet Explorer (IUE) Scientific Instrument (SI) (reference 2). NASTRAN (references 3 and 4) structural models (reference 5) were used as the basis for the thermal models, which were produced by a straight-forward conversion procedure. The accuracy of this technique was subsequently demonstrated by a comparison of \bar{N} TA predicts with the results of a thermal-vacuum test of the IUE Engineering Test Unit (ETU) (reference 6). Completion of these tasks was aided by the use of \bar{N} TA pre-and-post-processors and by a significant amount of program modification to NTA subroutines RMG and SSGHT.

INTRODUCTION

The NASTRAN program has quickly become a standard tool for the finite element structural analysis of large and/or complex structures. During this evolution it became apparent that the mathematical techniques employed in NASTRAN to solve structural analysis problems could be easily adapted to provide solutions to heat transfer problems (reference 7), with several major advantages accruing, in that:

(a) virtually the same finite element analytical model could be used for both cases;

(b) with the same analytical model being used for both structural and thermal analyses, thermal predictions could be

directly applied, with no error-inducing and/or time consuming interpolation, to the structural model to allow the calculation of thermally induced deformations.

An appealing concept, certainly, but concepts often run afoul of practical details and fail to ever be used effectively to produce the desired result of increased productivity. The intent of this paper is therefore basically to increase the steepness of the NTA learning curve by describing in detail the actual techniques used in converting an existing NASTRAN structural model into an executable NTA model. In support of this goal, information will be presented containing computer results, comparisons with test results, comments on effective analysis aids, and useful program coding modifications.

THE IUE SCIENTIFIC INSTRUMENT

Description

The IUE SI, as shown in Figure 1, consists of a Cassegrain telescope section and a spectrograph section, and as a whole is essentially an aluminum structure approximately 3 meters long and .7 meters in diameter. The prime purpose of this instrument is high resolution observation of stellar objects in the ultraviolet spectral region, and to this end tight optical tolerances of one arc-second resolution and less than one arc-second change in focus during a one-half hour observation were imposed. It was evident that the accurate optical performance analysis of this sensitive and complex system would require detailed structural and thermal models to provide the necessary predictions of optical component shifts due to thermally induced deformations. Given that detailed NASTRAN structural models of the telescope and the spectrograph already existed, the IUE SI clearly qualified as an ideal candidate for the first large-scale use of the NTA for flight project support.*

The NASTRAN Structural Model

Figures 2 and 3 are NTA plots of the major structure of the IUE telescope and spectrograph (plots of radiating elements were the most convenient to include here, but they are essentially

*The NTA was previously used to support the OSO project (reference 8), but that effort was essentially intended to test the integrated analysis concept for debugging purposes.

direct overlays of the planar structural elements). In combination these models consisted of 3006 degrees of freedom (reference 5), approximately 550 GRID points and 900 structural elements, and would seemingly be very difficult to convert to thermal models due to their sheer size and complexity. This problem is specifically addressed in the next section, where it will be assumed that the reader is familiar with the basic organization of a NASTRAN problem, and is aware that the NASTRAN User's Manual (reference 3) and the NTA Manuals (reference 1) may be consulted for detailed information on the implementation of any of the cited techniques.

GENERAL PURPOSE TECHNIQUE FOR THE CONVERSION OF A NASTRAN STRUCTURAL MODEL TO A NTA THERMAL MODEL

The following Sections are a general purpose statement outlining the techniques used to convert the IUE NASTRAN model to a NTA model.

Pre-modification

(1) Acquire a working understanding of the thermal design of the structure to be analyzed, with special attention being paid to areas with high power dissipations and/or crucial thermal contact couplings. It will often be the case that the structural model will be of insufficient detail in these areas, requiring additional modelling to be done.

This type of problem is too complex and non-general to be discussed in detail in this paper, as it falls into the category of engineering judgement;

(2) Obtain NASTRAN element and GRID point structure plots similar to those in Figures 2 and 3, along with a verbal description of the model including materials used and simplifying assumptions;

(3) Decide whether NLSS or NLTR results are required (linear problems may be solved by the same solution algorithms, or, for linear steady-state problems, a special algorithm is available). The conversion technique presented will initially produce a NLSS model, but the further changes required to produce a NLTR model will also be described.

Card Removal

Using a punched deck copy of the NASTRAN structural model:

- (1) Remove the Executive and Case Control Decks;
- (2) Remove all Bulk Data Deck cards except GRID, SPOINT, connection, property, coordinate, relevant \$, GRDSET, BAROR, SEQGP, BEGIN BULK, and ENDDATA cards (the thermally acceptable connection cards are listed in the NTA Manual (reference 1));
- (3) Remove any permanent constraints defined on GRID cards or on a GRDSET card.

This reduced structural model Bulk Data Deck is now ready for conversion to a NTA model.

NLSS Card Additions

Using the card deck generated in the previous section:

- (1) Add Case Control and Executive Control Decks;
- (2) If degree-of-freedom information is requested by a card-type, always use 1;
- (3) Add MAT4, MATT4, MAT5, and/or MATT5 cards to define thermal conductivities (eg - $\bar{W}/m-^{\circ}C$) for each material type referenced by the property cards in the model;
- (4) If any CELASi cards are present, examine them to determine, based on their location in the structure, what effective conductance (eg - $W/^{\circ}C$) should be entered in field 3 of each card;
- (5) List on an SPC1 card all GRID points which are to be held at fixed temperatures;
- (6) If any GRID points are to be maintained at equal but unspecified temperatures, list them on one or more MPC cards (more complex temperature relationships may be defined if none of the GRID points involved are subject to non-linear effects);
- (7) If any MPC, SPC, or permanent constraints were removed from the structural model, carefully examine the GRID points affected to verify that they are satisfactorily coupled into the thermal model;
- (8) Define a temperature "guess vector" consisting of TEMP

cards and/or a TEMPD card. All GRID points in the model must have a guess temperature, and those GRIDS listed on an SPC1 card will be constrained to that temperature. In addition, to assure convergence, all guess temperatures should be no less than 80% of the final steady-state absolute temperature of the respective GRID points;

(9) Define a thermal load vector if heat is to be applied to any elements or GRID points;

(10) If radiative, convective, and/or contact heat exchange is to be allowed, CHBDY elements and supporting property and/or material cards must be added to define the active surfaces. In addition, if gray body radiative couplings are present, RADLST and RADMTX cards are required to, respectively, define the radiatively active CHBDY cards, and the area-times-view-factor coupling (eg-m²) between the active CHBDY cards;

(11) Add four PARAM cards (EPSHT, MAXIT, TABS, and SIGMA) to define, respectively, the convergence criteria, the maximum number of iterations, the absolute temperature conversion factor (eg-273.15 for °C), and the Stefan-Boltzmann Constant.

This completes the basic Bulk Data Deck changes required to produce a NLSS NTA deck from a NASTRAN structural model.

Further NLTR Card Additions

The NLSS Card deck produced in the previous section may be converted to a transient form if the following changes are made:

(1) Minor modifications to the Executive and Case Control Decks are required;

(2) Proper thermal masses (eg-J/°C) must be applied to the GRID points in the model. This is done primarily through specifying a volume thermal mass (eg-J/m³-°C) on the thermal material cards. Additional thermal mass may be applied through the use of CVISC and/or CDAMPi cards. The CHBDY card may also be used to provide thermal mass in conjunction with convection (½ of the thermal mass specified will be applied to the ambient point(s)). Note that structural mass has no relationship to thermal mass,* with the correct analogy equating viscosity or damping with thermal mass. Singular thermal mass matrices are allowed, but my experience has been that stability is somewhat impaired;

*Non-structural mass from the structural model will not supply any thermal mass.

(3) All thermal loads must be referenced via TLOAD1 and/or TLOAD2 card(s);

(4) An "initial condition" temperature set composed of TEMP cards and/or a TEMPD card must be supplied. The thermal "guess vector" used in the NLSS model should still be used, as it appears to improve the stability of problems with singular thermal mass matrices (for an oscillating solution, good results are obtained with a guess at approximately the average solution value);

(5) MPC's are unaffected, but SPC's may only be used to constrain GRID points to 0°. They must be replaced with the well-known "ground-and-load" system* which allows both fixed temperatures and fixed time/temperature histories to be specified;

(6) A TSTEP card must be added to specify the number of integration time steps, their length, and the frequency of output;

This completes the Bulk Data Deck changes required to convert a NLSS NTA model to a NLTR one.

IUE THERMAL PREDICTS vs TEST RESULTS

These procedures were followed to transform the structural models of the IUE telescope and spectrograph into a complete NLSS NTA model (reference 9). A comparison at representative points of the predicts generated by this model with the actual results of an ETU thermal vacuum test (reference 6) performed at the Goddard Space Flight Center is presented in Table 1, and is accompanied by the thermal predicts produced by the post-test updated model (reference 10). Agreement was in general excellent, with the major differences being traced to incorrect coating assumptions in the area of the secondary mirror and incorrect joint conduction assumptions at several points in the model.

ANALYSIS AIDS

In the course of using any program extensively, one slowly acquires a collection of especially effective or useful analysis aids or techniques which through lack of documentation and/or lack of general usage are not obvious to the new user. The following four items, all used in the IUE analyses, fall into this category and should prove useful to most NTA analysts.

*See Reference 1

The VIEW Program (references 11 and 12)

This program is designed to automatically produce the RADMTX and RADLST cards required to simulate diffuse radiative interchange, including shading, between CHBDY elements. As input, it requires primarily the same CHBDY, PHBDY, and GRID cards used in the NTA model, with one additional card type being used to specify mesh sizes and optional shading information. VIEW is currently operational on IBM 360-370 series computers (but could be converted to UNIVAC or CDC operation in roughly one month) and executes in as little as 110K decimal 8-bit bytes from an overlaid load module occupying 26 7294-byte tracks. VIEW was found to be vital to the IUE NTA analyses as it greatly simplified the required computation and correction of the large view factor matrices involved.

Modelling Multi-Layer Insulation (MLI)

A common problem in thermal modelling is how to account for MLI. If it is assumed that the heat loss through the MLI cannot simply be completely neglected, two methods are suggested:

(1) Effective emissivity. The NTA assumes that the information entered on the RADMTX cards is area-times-view-factor for gray bodies, rather than Script-AF data. Therefore the use of effective emissivity is approximately valid only when the CHBDY card using an effective emissivity sees only essentially black fixed temperature surfaces (such as the outside of the IUE Telescope looking at space). Also, of course, an effective absorbtivity would have to be specified to account for external inputs such as solar energy.

(2) Effective conductance per unit area. This is a more straight-forward technique, and requires that the analyst estimate the effective conductance through the MLI over a unit area (eg-W/m²-°C) and assume that the CHBDY cards are on the outer layer of the MLI.* The emissivity and absorbtivity of the CHBDY cards would correspond to that of the outer surface of the MLI, and convection would be defined from the same CHBDY cards to the GRID points on the structure directly beneath the MLI, with the convective coefficient "h" corresponding to the effective conductance per unit area through the MLI (see Figure 4). This method is obviously much more flexible than the one previously described, as there are no constraints on the surroundings nor is there any need to calculate an effective absorbtivity. However, care must be taken to ensure that, for both NLSS and

*New GRID points must be defined for these elements.

NLTR runs, the thermal "guess vector" is appropriate for the GRID points associated with the CHBDYs on the MLI, or instabilities will result.

Solution and Transient Printer Plotting of Linear Equations

Early in the IUE analyses simple, linear parametric equations were developed relating the defocus of the telescope to factors such as axial and circumferential thermal gradients, changes in mirror temperatures, etc. It became apparent that these equations could be solved during a NTA run by adding new GRID points whose values would be appropriately defined by MPCs. It would also be possible to use the NTA printer-plotter, if the run were a transient, to plot the value of the GRID point which represented defocus as a function of time (see Figure 5*). This "on-line" analysis technique would obviously be applicable to all forms of linear equations and provides an excellent quick-look for the analyst faced with an otherwise difficult to peruse stack of NTA output.

On-Line NTA Post Processors

When a large NTA model is to be run more than 10-15 times, a problem can develop with respect to actually examining the enormous volume of data which is generated. While transient plotting will help to some degree, an on-line post processor may be a better answer, as was found to be the case for the IUE analyses.

The method is quite simple, and involves requesting temperature, load, and constraint power output in punched as well as printed format (eg-OLOAD (PRINT, PUNCH) = ALL). The punched card images are sent to a direct-access storage unit instead of a card-puncher, and when the NTA execution is complete, a user written FORTRAN program may be compiled and executed in-line to read the card images and print out neatly formatted summaries of the results for the job. Figure 6 shows the format of sample punched temperature, load, and constraint force cards, while Figure 7 shows an actual automatically and immediately generated summary report.

*A defocus/time plot from the NTA OSO analyses (reference 8) is shown as it was the more reproducible of the plots available.

PROGRAM MODIFICATIONS

During the course of the IUE thermal analyses, it became obvious that several relatively minor improvements to the $\bar{N}TA$ coding would allow a considerable increase in the program's efficiency, capability, and "useability." Since inclusion of the actual FORTRAN code changes would be too lengthy for this presentation, discussion will be limited to an outline of the use of the new features and the $\bar{N}TA$ subroutines which were modified to implement them, with the understanding that more complete information can be obtained from either Mr. Clifton E. Jackson, Jr. or Mr. Reginald S. Mitchell, Code 720.2, Goddard Space Flight Center, Greenbelt, Maryland 20771.

Additional "Space Node" Flexibility

An option was supplied to allow elimination of the automatic assumption that any energy not accounted for in the RADMTX should be discarded (the so-called "space node" feature). The new option, if elected, would assume that energy not accounted for would be returned to the element from which it was radiated. Additional related features added included the capability to partition the RADMTX into "space node" and "non-space-node" portions, and a summation check to assure that the RADMTX does not in effect specify emissivities greater than 1.0. The addition of these features required modifications in subroutine RMG only.

Script-AF Input

The original $\bar{N}TA$ required the use of an internal Script-AF generator in order to include radiative interchange, a fact that prevented the use of externally generated Script-AF matrices. A modification to subroutine RMG now optionally allows either symmetric or unsymmetric Script-AF matrices to be input to the $\bar{N}TA$ using the standard RADMTX and RADLST cards.

Symmetric Decomposition

When the full-scale NLSS model of the IUE experiment was first run, CPU and I/O solution times on the order of an hour were observed. An examination of the run logs for this problem indicated that large amounts of time were being spent in the unsymmetric decomposition of symmetric radiation and conductance matrices. It was determined that minor limitations on input (emissivities not equal to exactly 1.0, and uniform thermal guess

vectors for unconstrained GRID points if radiative interchange were included) would allow the use of symmetric decomposition in both cases. Modifications were made to subroutines RMG and SSGHT, an additional parameter was added, and run times were cut to less than 18 minutes CPU and I/O, with only round-off error changes in the answers produced. A similar conductance matrix decomposition feature was later added for transient runs, and it appears that it would be especially useful if time step sizes were changing frequently.

CONCLUDING REMARKS

The NTA has been used to provide thermal analyses of the IUE SI using structural models as the analytical baseline. The verification of this technique via test has demonstrated the accuracy of the NTA as a thermal analytical tool, and the analysis aids and program modifications listed will assist in making it a useful one.

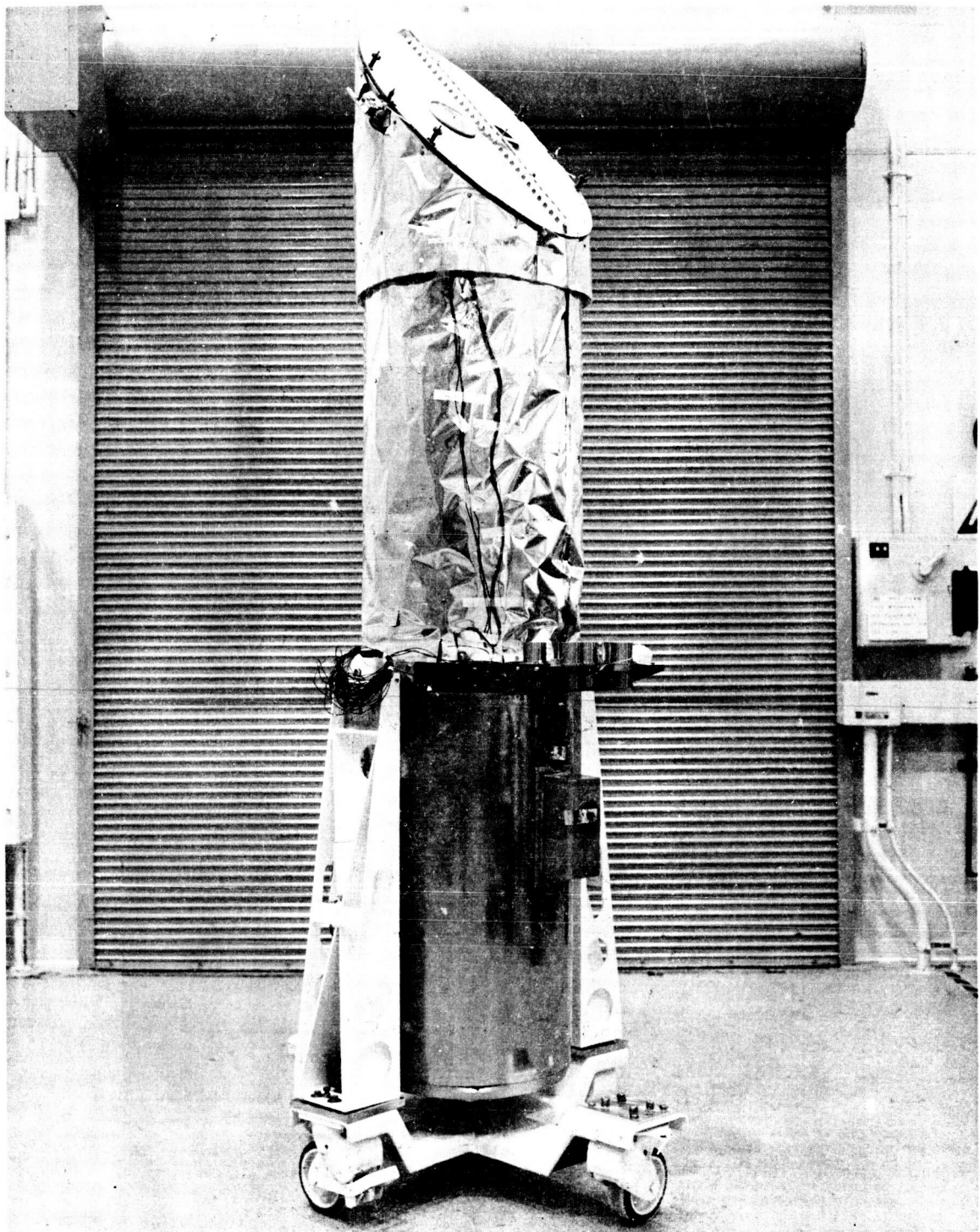
REFERENCES

1. Lee, Hwa-Ping; Jackson, Clifton E., Jr.: NASTRAN Thermal Analyzer - Theory and Application Including a Guide to Modelling Engineering Problems (2 Volumes). NASA-Goddard Space Flight Center X-322-76-17, December, 1975.
2. System Design Report for the International Ultraviolet Explorer (IUE) - Volume I - Scientific Instrument. NASA-Goddard Space Flight Center, June, 1973.
3. MacNeal, R. H. (Editor): The NASTRAN Theoretical Manual. NASA SP-221, with Level 15.5 updates, December, 1972.
4. McCormick, C. W. (Editor): The NASTRAN User's Manual (Level 15). NASA SP-222(01), with Level 15.5 updates, June, 1972.
5. Case, William R.: Dynamic Substructure Analysis of the International Ultraviolet Explorer (IUE) Spacecraft. NASA TM X-3278, 1975, pp.221-248.
6. Seivold, A. L.: International Ultraviolet Explorer Engineering Test Unit - Final Report of the IUE-ETU Thermal Balance Test. NASA-Goddard Space Flight Center-Test and Evaluation Division Report #03169, December, 1975.
7. Mason, James B.: The Solution of Heat Transfer Problems by the Finite Element Method Using NASTRAN. NASA-Goddard Space Flight Center X-321-70-97, February, 1970.
8. Lee, Hwa-Ping; Jackson, Clifton E., Jr.: A Summary of the STOP Thermal Analysis of the OSO-I Colorado Experiment. NASA-Goddard Space Flight Center-Test and Evaluation Division Report #03064, April, 1974.
9. Jackson, Clifton E., Jr.: A Summary of the NASTRAN Thermal Analyses Performed on the IUE Scientific Instrument From 1-1-74 to 7-23-75. NASA-Goddard Space Flight Center X-322-75-306, August, 1975.
10. Jackson, Clifton E., Jr.: Verification of the NASTRAN Thermal Analyzer (NTA) Model of the IUE ETU Scientific Instrument. NASA-Goddard Space Flight Center, Test and Evaluation Division Memorandum to J. B. Mason, July 7, 1975.
11. Puccinelli, E. F.: View Factor Computer Program (Program VIEW) User's Manual. NASA-Goddard Space Flight Center X-324-73-272, July, 1973.

12. Jackson, Clifton E., Jr.: Programmer's Manual for VIEW-
A Modification of the RAVFAC View Factor Program for Use
With the NASTRAN Thermal Analyzer on IBM-360 Series
Computers. NASA Goddard Space Flight Center X-322-73-120,
March, 1973.

TABLE I - CORRELATION OF THE IUE TEST AND THE ANALYTICAL MODELS

Location	$\beta = 0^\circ$ (no sun on telescope)			$\beta = 90^\circ$ (sun angle perpendicular to telescope)		
	Test °C	Unverified model °C	Verified model °C	Test °C	Unverified model °C	Verified model °C
Secondary mirror baffle	-59 to -65	-50 to -51	-53 to -59	-52 to -58	-48 to -49	-47 to -53
Primary mirror baffle	-20 to -41	-23 to -42	-23 to -47	-14 to -34	-20 to -40	-18 to -41
Primary mirror	-7 to 1.3	1.0	1.2	3.1 to 5.4	3.5 to 3.6	5.5
Focus drive mechanism	-40	-29	-38	-33	-28	-32
Secondary mirror	+13 to +18	-22	+13	16 to 21	-20	17
ACQ camera #1	+4 to +5	1.7	3.5	8 to 10	4	8
LWL camera #1	+6 to +9	2.2	4.1	11 to 13	5	8
SWL camera #1	+6 to +8	1.7	3.9	11 to 13	4	8
Fine error sensor sensor	+3 to +9	3	8	7 to 14	6	12
Fine error sensor electronics	+4 to +5	1	2	9	3	6
Acquisition deck	0 to +1	-2	-1.3	5 to 6	.5	3
Aperture deck	0	-1.0	-.7	4 to 5	1 to 2	3 to 4
Camera deck	3	1.5	1.7	7 to 8	4	6
Echelle deck	+3 to +4	.8	2.6	7 to 9	3 to 4	6 to 7
Collimator deck	+6	1.3	3.8	10	4	8
Sunshade	-98 to -112	-87 to -91	-95 to -106	-85 to -100	-76 to -86	-82 to -100
Tube	-20 to -64	-17 to -56	-18 to -60	-14 to -57	-14 to -55	-12 to -54
Strong ring	-16.8 to -17.8	-17.1 to -17.9	-17.3 to -18.4	-10.8 to -12.4	-13.1 to -14.3	-11.9 to -13
Spectrograph dust cover	-12 to +5	-7 to +2	-7 to +5	-7 to +9	-5 to +4	-2 to +8



NASA G-75-05232

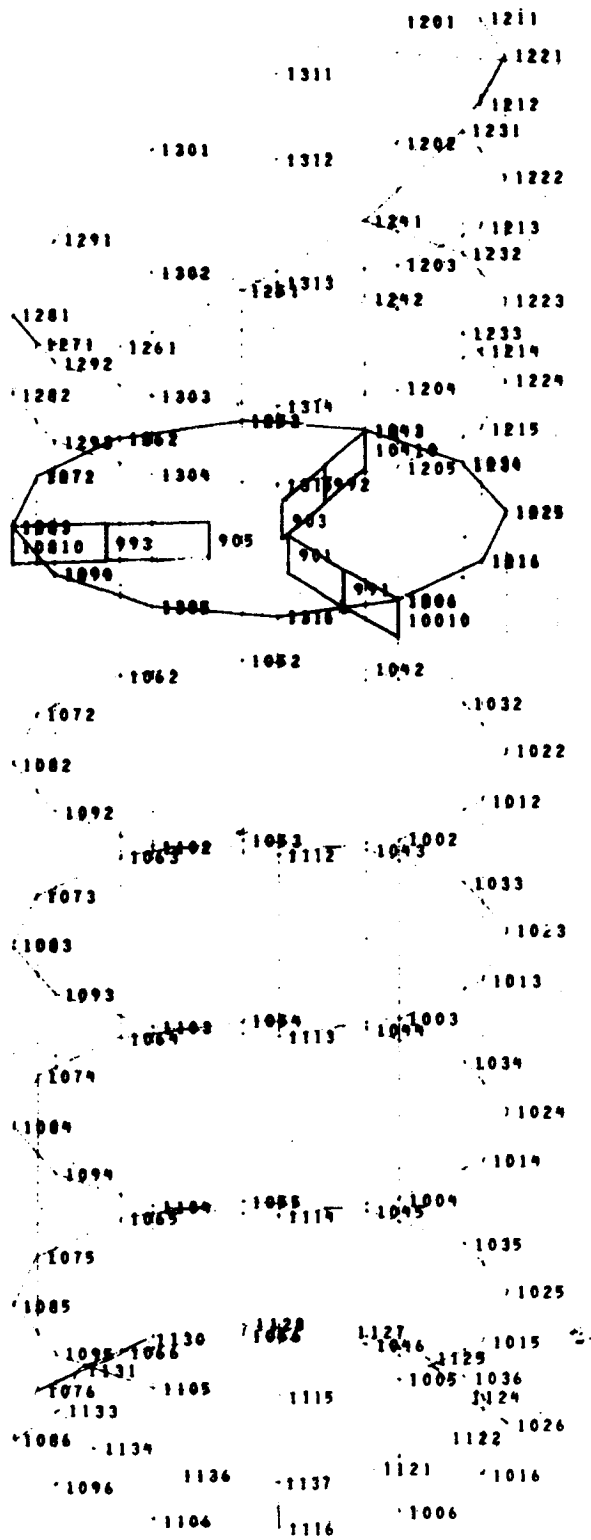


Figure 2. NTA Plot of the Major IUE Telescope Radiating Elements

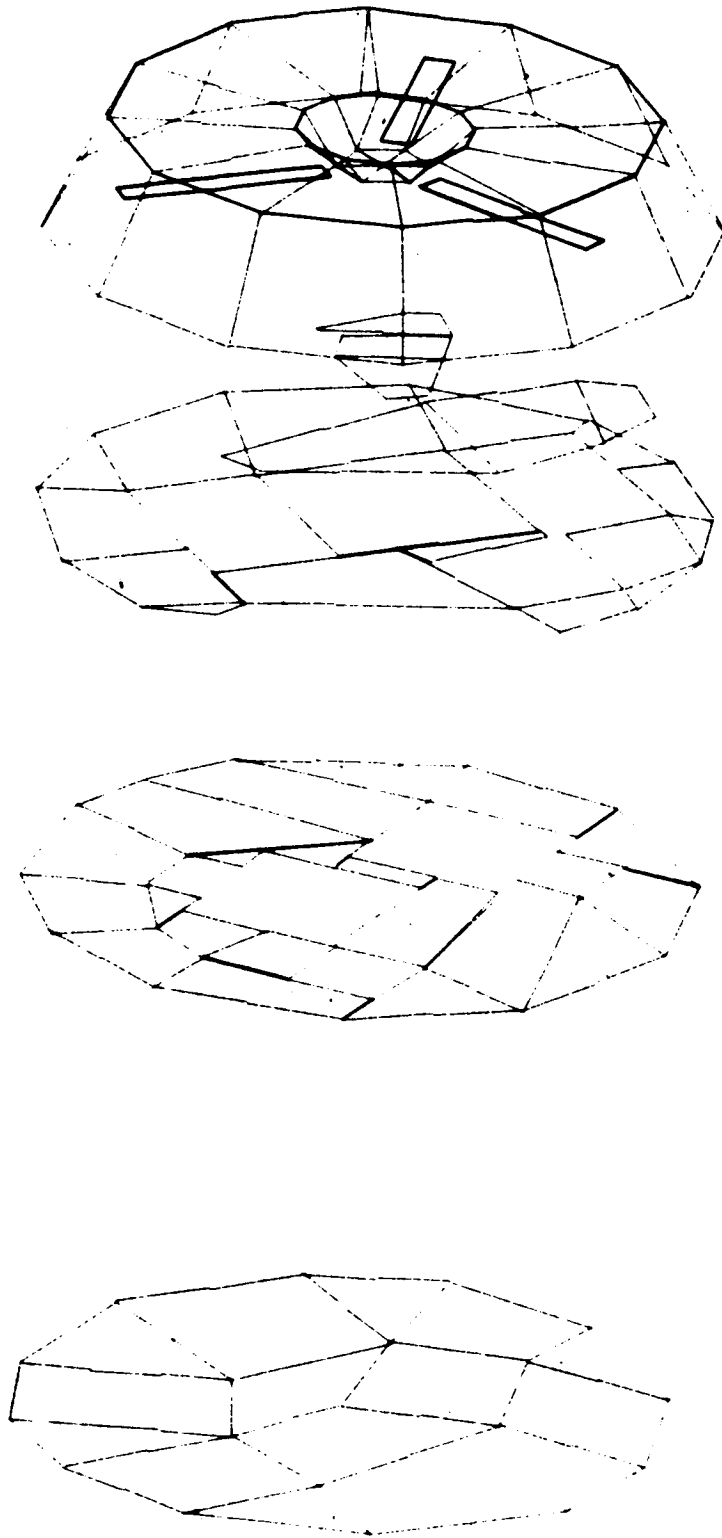


Figure 3. \bar{N} TA Plot of the Major IUE Spectrograph Deck's Radiating Elements

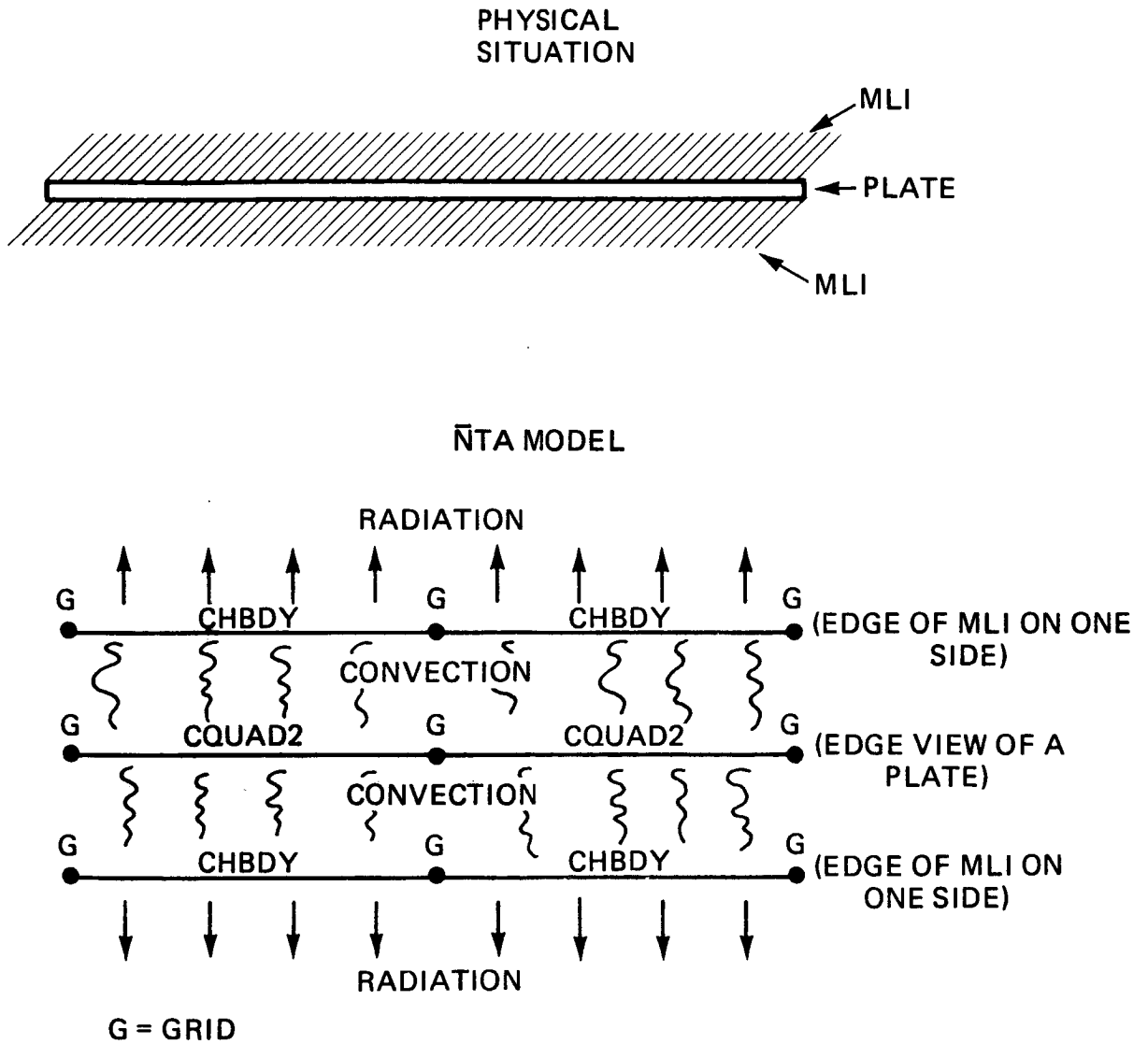
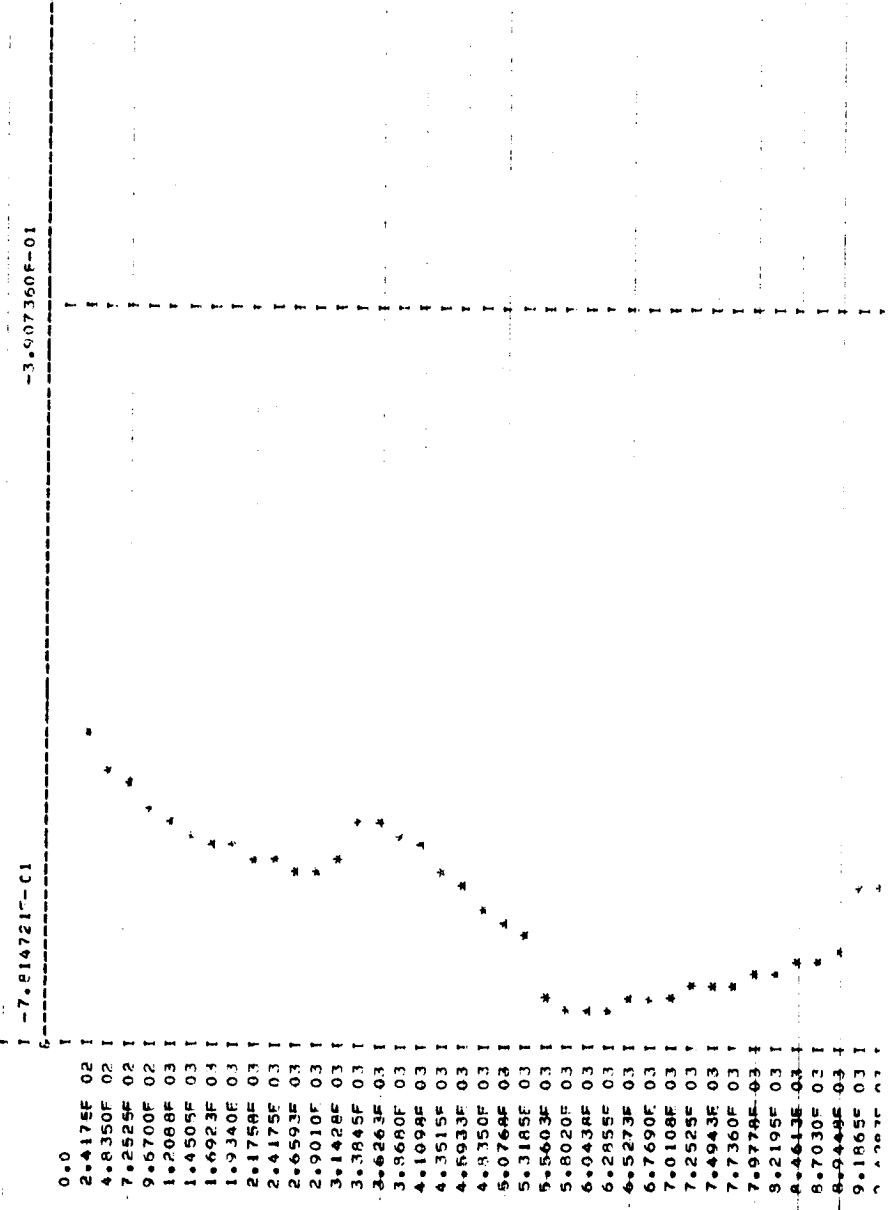


Figure 4. Outline of One Method of \bar{N} TA MLI Modeling

X-AXIS TITLE = ORBIT TIME (SECONDS) --- ONE COLD ORBIT = 5902 SECONDS

Y-AXIS TITLE = DEFOCUS IN ARC SECONDS



7.814721E-01

-3.907360E-01

-1.387779E-17

Figure 5. NTA Plot of Defocus (vs) Time for the OSO Telescope

TITLE = IUE EXPERIMENT THERMAL MODEL --- 10/31/74
 SUBTITLE = SPACECRAFT, PM AND SM, AND SPACE AS BOUNDARIES
 LABEL = TEST RUN OF THE COMBINATION PROCEDURE

DISPLACEMENTS
 REAL OUTPUT
 SUBCASE ID = 1 1 1
 607 -4.821902E 01
 608 -3.757886E 01
 609 -3.757886E 01

TITLE = IUE EXPERIMENT THERMAL MODEL --- 10/31/74
 SUBTITLE = SPACECRAFT, PM AND SM, AND SPACE AS BOUNDARIES
 LABEL = TEST RUN OF THE COMBINATION PROCEDURE

LOADS
 REAL OUTPUT
 SUBCASE ID = 1
 611 S 1.0595959E C0
 612 S 8.200000E-01 C.C
 613 S 8.200000E-01 C.C
 1001 S 1.003368E-01 C.C
 1002 S 1.760916E-01 C.C
 0.0 C.C

TITLE = IUE EXPERIMENT THERMAL MODEL --- 10/31/74
 SUBTITLE = SPACECRAFT, PM AND SM, AND SPACE AS BOUNDARIES
 LABEL = TEST RUN OF THE COMBINATION PROCEDURE

SPCF
 REAL OUTPUT
 SUBCASE ID = 1
 6000 S 2.920006E-04 0.0
 6091 S -1.870287E-02 0.0
 8092 S -1.703292E-02 0.0
 9093 S -2.009553E-02 0.0
 9094 S -1.684505E-02 0.0
 0.0 0.0

1
2
3
4
5
6
7
8
9
10
11
12

818
819
820
821
822
823

824
825
826
827
828
829
830
831
832
833
834
835
836

1071
1072
1073
1074
1075
1076
1077
1078
1079

1080
1081
1082
1083
1084
1085
1086
1087
1088
1089

Figure 6. Partial IUE Punched Temperature, Thermal Load, and Constraint Force Output

```

SECONDARY MIRROR AXIAL
-----
SECONDARY MIRROR
SECONDARY MIRROR AXIAL DELTA T =
FOCUS DRIVE
IMAGE STAGE
CENTER OF VANE
OUTER RING
MAXIMUM DELTA T ON CUTTER RING
MINIMUM RAFFLE
MAXIMUM RAFFLE

GENERAL
-----
MINIMUM SUNSHADE =
MAXIMUM SUNSHADE =
AVERAGE SUNSHADE =
AVERAGE AXIAL TUBE DELTA T =
INCLUDING RINGSE
EXCLUDING RINGSE

PRIMARY MIRROR APPA
-----
PRIMARY MIRROR =
MAX P.W. AXIAL DELTA T =
AVERAGE TANGENT HAZE
STRONG RING
MAXIMUM DELTA T ON STRONG RING
MINIMUM RAFFLE
MAXIMUM RAFFLE
MAIN RAFFLE SURFDATE

POWER SUPPLIED
-----
SECONDARY MIRROR 2.74
PRIMARY MIRROR 5.00
ISA 0.00
1/2 C/T STRONG RING 5.30
SCALAR INPUT 4.28

* SPECTROGRAPH TEMPERATURES *

POST CURVE
-----
THETA T W MID BOTTOM JACK
0-120 DEG -3.3 3.7 5.8 5.2
120-240 DEG -1.9 2.8 5.9
240-360 DEG -1.9 3.6 5.7
S/C ATTACH B= C 12.0
S/C ATTACH B=138 12.0
S/C ATTACH B=228 12.0

SPACECRAFT
-----
0-120 DEG 14.0 14.0 17.0
120-240 DEG 14.0 5.0 17.0
240-360 DEG 14.0 14.0 17.0

APERTURE ACQUISITION DECKS
-----
0.8
0.1
1.6
7.4

CAMERA
-----
2.4
1.5

FCHLLE
-----
4.7
C.3

COLLIMATOR
-----
6.0
0.1

AVERAGE TEMPERATURE =
MAXIMUM DELTA T =

LWL
-----
5.6
3.5

FESS2
-----
3.1
7.3

ECHELLE
-----
4.4
4.4

COMPONENTS
-----
SWL
5.7
3.0

FESS1
-----
7.3

FCHLLE
-----
4.7
C.3

COLLIMATOR
-----
6.0
0.1

TOTAL EXPERIMENT ENERGY SUMMARY
-----
WATTS IN 3.0 WATTS OUT 0.0 PER CENT ERROR 0.0
WATTS TO SPACE 29.24

* SPECTROGRAPH ENERGIES *
-----
SWL
4.44
0.00
TOTAL SPECTROGRAPH 11.46
S/C ATTACH B= C JUST COVERED 9.57
S/C ATTACH B=138 0.21
S/C ATTACH B=228 0.21

```

Figure 7. Sample Automatic Post-Processor Summary Report for the IUE SI